

# Multispectral Image Correction for Geometric Measurements

M Rosenberger<sup>1</sup>, G Linß<sup>1</sup>

<sup>1</sup>Ilmenau University of Technology, Department Quality Assurance and Industrial Image Processing, Gustav Kirchhoff Platz 2, 98693 Ilmenau, GER

maik.rosenberger@tu-ilmenau.de

**Abstract.** Multispectral- and hyperspectral imaging technologies enable new possibilities in industrial measurement applications. Based on the knowledge of remote sensing a lot of investigations were made in the last decades of years. Nevertheless the demands on remote sensing versus technical multi spectral image processing are quite different. In the field of precise geometric measurement technics it is necessary to correct the image data between different spectral channels with a high accuracy, normally in the micron range. Otherwise the geometric absolute value of fail detection on edges can be become very large. State of the art in industrial imaging and detection of geometric features is the calibration of only one imaging channel. In this paper, the studies on a twelve channel multi spectral imager were presented. For the applied filter wheel system, investigations on the improvement of lens aberration as well as for the defocus problem were made. Therefore a calibrated high precision geometric test chart was used to calibrate the system geometrically. To correct the geometric errors on the image plane a special moving filter approach, based on linear convolution, was developed. For every channel a calibration matrix were calculated and applied on the image system output.

## 1. Introduction

The analysis of space resolved spectral information is only possible to a certain limit with an ordinary colour camera [1],[2].

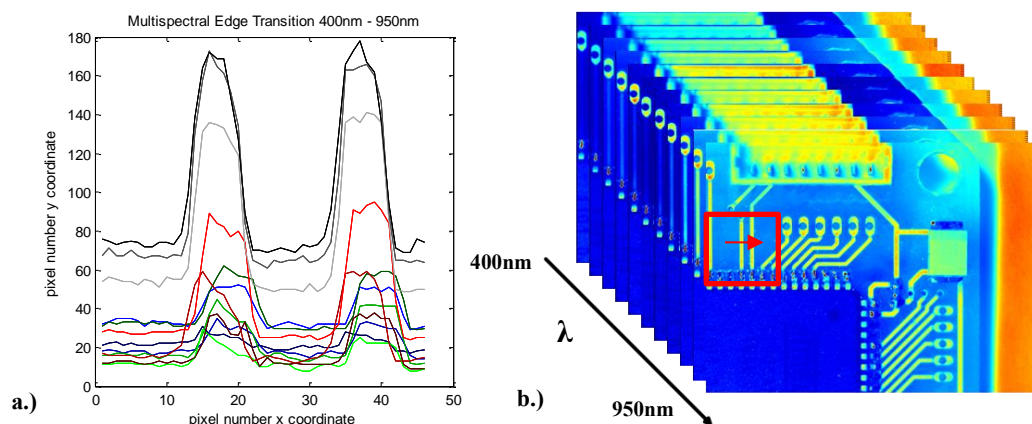


**Figure 1:** a.) multi spectral edge transition, along the search line (red arrow) of a twelve channel spectral cube (b.); (blue graphs 400-500nm, green graphs 550-650nm, red graphs 700-800 nm, grey scaled graphs 850-950nm);

The technical function principle of ordinary Red Green Blue (RGB) cameras with a maximum of three colour channels can dissolve only a limited range in the colour space and loose spectral image



information. The comparatively large sensitivity of the three individual colour channels results to lose some spectral information. A multispectral camera operates with several colour channels and reconstructs a complete spectrum with specific numerical methods. Filter wheel cameras present an effective and affordable alternative in multispectral image acquisition Figure 2 [3],[4].

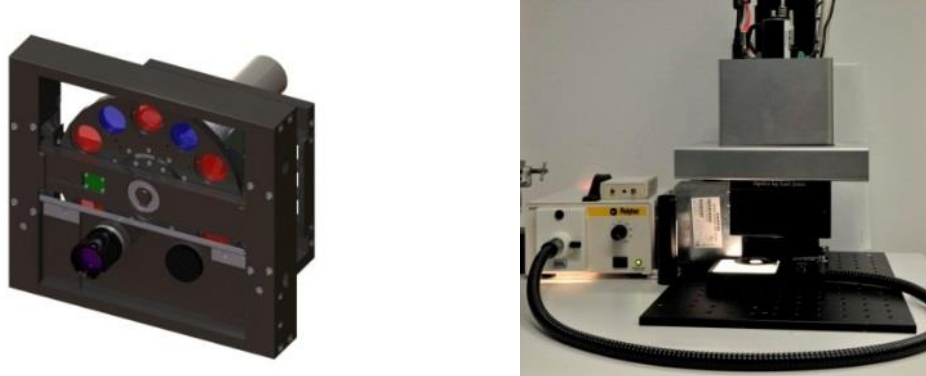


**Figure 2: multispectral imager 3D-model and inside view on the left, assembled twelve channel multispectral imager on the right;**

Their modular and versatile structure, as well as the consistent enhancements in filter and sensor technology offer many pros for use of these systems. Actually a lot of investigations were made to increase the spectral resolution for space resolved spectral imaging systems. The simultaneously data acquisition of the complete two dimensional field is not solved already. Only push broom scanners can capture spectral images like a line camera. Filter wheel cameras do not have that problem but during the filter exchange it loss information of fast moving object scenes. Every technology has its pros and cons depending on the application. As well as the resolution in wavelength, for geometric measurement an accurate correction of aberrations are necessary to achieve lowest measurement uncertainties. That leads to a correction of every spectral channel. The need for the transfer of multispectral imaging technologies in industrial application is to make features visible that actually cannot be detected with greyscale or RGB –imaging. Figure 1 shows a multispectral cube captured with a filter wheel camera [3] and the information along a search line in all channels. There is lot of complicated measurement tasks for industrial measurement especially in the field of injection moulded parts and composite technologies. In the following the imaging setup will be presented partly and a short introduction of wavelength depended aberrations for spectral imaging is given.

## 2. Challenges in Multispectral Image Acquisition

The two major challenges in multispectral imaging are the increase of wavelength stability and wavelength resolution as well as the increase in spatial resolution. Therewith it is essential to calibrate the system. In many publications a model based correction is described mostly for applications in bio science and remote sensing. In the case of precision measurements the goal should be a very small amount of residue. With that the problem is that the most lenses are corrected in three wavelengths in the RGB range. Based on the longitudinal aberration in diffractive optics the focus point of every wavelength channel is located on a different position and must be corrected. The spot size in the image plane differs from the focused wavelength (minimum spot size) up to 10 microns (Figure 4 a.) This effect is based on the different propagation wavelength in materials. A possibility to correct this aberration is to enlarge the optical path of light specifically. Therefore the sellmeier equation with the sellmeier coefficients were used to calculate the thickness of the correction plates [5]. First the wavelength dependent refractive index can be calculated by equation 1.

$$n(\lambda) = \sqrt{1 + \frac{B_1\lambda^2}{\lambda^2 - C_1} + \frac{B_2\lambda^2}{\lambda^2 - C_2} + \frac{B_3\lambda^2}{\lambda^2 - C_3}} \quad (1)$$

With the knowledge about the wavelength dependent refractive index and the assumption of an additional way for the propagating light the following equation 2 leads to the thickness of the correction plates  $dl_\lambda$ .

$$dl_\lambda = \frac{df_\lambda n_{\lambda,BK7}}{n_{\lambda,BK7} - n_{\lambda,air}} \tag{2}$$

To calculate the thickness of the correction plates the focus deviations have to be measured in the optical path or have to be simulated. To consider the tolerances in the complete optical path like the tolerances in the lens, the tolerance in the lens mountings, the tolerances in the filter mountings and as well as the tolerances in the sensor mounting, the focus shift were measured inside the system on all twelve filter wavelengths. For this reason a calibration chart were used to get sharp edge transitions. The contrast values on the edge transition were evaluated. On the contrast maximum the optimal focus position will be expected. To realize the focus procedure a high precision linear bearing with a measurement system which resolves up to 10 microns were adapted into the camera system. The adjustable motion system carries the image sensor and can be moved for the measurement very precisely. The results of the measurements of the wavelength depended focus shift is given in Figure 3. The start position of the focus position was placed in the infrared region.

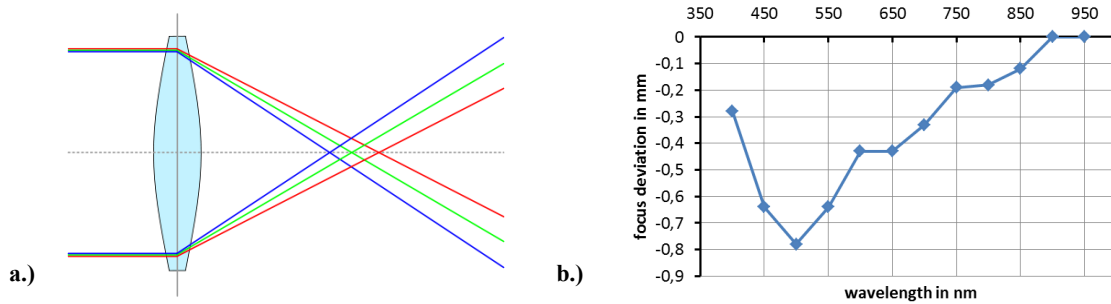


Figure 3: a.) schematic of wavelength dependent focus deviation, b.) measured focus deviation on the image plane (image sensor ICX 415AI lens: Distagon 2,8/25 ZF IR);

From that position a linear trend were expected. This trend can be observed until 550nm (Figure 3). Below 550 nm the trend distance to the start position increases. This effect can be traced back to a deviation of thickness of the color filters as well as of the chromatic lens optimization in the RGB-Range. At the end a range between 150 microns up to 2000 microns were calculated for the correction of the entire wavelength range for the used lens.

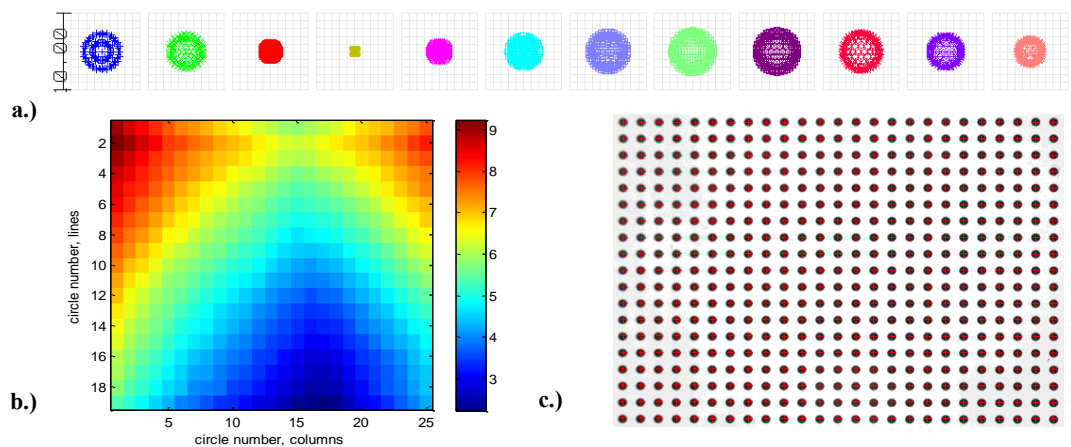


Figure 4: a.) optical simulation of longitudinal aberration of an apochromat, beginning from the 400nm band in steps of 50nm, base wavelength 550nm; b.) maximum field aberration between all channels of the test target (the colour value is the aberration in pixel); c.) calibrated test chart with detected centre points;

With the knowledge of the thickness for the different correction plates the focus shift were compensated. The mounted correction plates generating an additional optical lateral shift which have to be corrected on the image plane. This optical shift and the distortion of the lens give the absolute error on the image plane. With the calibration test chart (pitch 1000 $\mu\text{m}$ , Figure 4 c.) the maximum measured deviation between the different wavelength ranges is nine pixels. The spatial error distribution is displayed in Figure 4 b.). To calculate the complete distortion the following procedure was developed. After the correction with the calculated correction plates, the focus shift is strong minimized, so every filter were evaluated separately. To extract the circles in the image a Hough-Transformation was used. At the end of the applied transformation a table with x and y coordinates were generated. After that the approach of an minimal distortion in the middle of the lens were assumed. With this assumption the five circles in the idle of the image were used as the reference. Furthermore the distance of the different circles of the calibration target in the image are known. With the knowledge of the reference positions of the calibration targets an reference matrix of circle points were calculated. The difference between the x- and y-coordinates leads to the deviations in the separate directions. Furthermore the pixel factor can be calculated with this data. At the end an deviation cube of 19 x 25 x 12 data points were processed for the correction algorithm. In case of another lens only the size have of the matrix have to be changed.

### 3. Approach for Correction

Based on the measured centre points (Figure 3. b-c.) the deviations from the expected positions of the centre points can be calculated for every channel. For this operation a polynomial with an grade of three were used to fit the discrete values into an continuous function. With x the measured position in the column direction (x) and  $a_x$ - $d_x$  the polynomial coefficients leads to the approach (equation 3):

$$f(x_c) - x = a_x x^3 + b_x x^2 + c_x x + d_x \rightarrow \min \quad (3)$$

After the optimization the four coefficients for every column in 19 lines were done. That leads to an matrix with nineteen  $a_x$ ,  $b_x$ ,  $c_x$ ,  $d_x$  coefficients. Furthermore the calculated coefficients  $a_x$ - $d_x$  can be described also as continuous functions in the line direction (y) (equation 4-7):

$$f(a_x) - a_x = a_{y3} y^3 + b_{y3} y^2 + c_{y3} y + d_{y3} \rightarrow \min \quad (4)$$

$$f(b_x) - b_x = a_{y2} y^3 + b_{y2} y^2 + c_{y2} y + d_{y2} \rightarrow \min \quad (5)$$

$$f(c_x) - c_x = a_{y1} y^3 + b_{y1} y^2 + c_{y1} y + d_{y1} \rightarrow \min \quad (6)$$

$$f(d_x) - d_x = a_{y0} y^3 + b_{y0} y^2 + c_{y0} y + d_{y0} \rightarrow \min \quad (7)$$

At the end of the calculation of all coefficients the deviation can be described with sixteen coefficients for every channel. For the calculation of the corrected position the following equation 8 was derived:

$$\begin{aligned} dx = & (a_{y3} y^3 + b_{y3} y^2 + c_{y3} y + d_{y3}) x^3 + \\ & (a_{y2} y^3 + b_{y2} y^2 + c_{y2} y + d_{y2}) x^2 + \\ & (a_{y1} y^3 + b_{y1} y^2 + c_{y1} y + d_{y1}) x + \\ & (a_{y0} y^3 + b_{y0} y^2 + c_{y0} y + d_{y0}) \end{aligned} \quad (8)$$

The same procedure has to be applied for the y coordinate correction of the image. The approximations of the discrete coefficients versus the discrete coefficients are graphical displayed in the following Figure 5. For every pixel the two correction values gives information about the direction and the amount of deviation. With the approximation for the y and x direction of the deviations of the circles on the calibration target a very precise correction can be calculated for every pixel. Therewith up to four pixels have to be weighted to generate the result pixel.

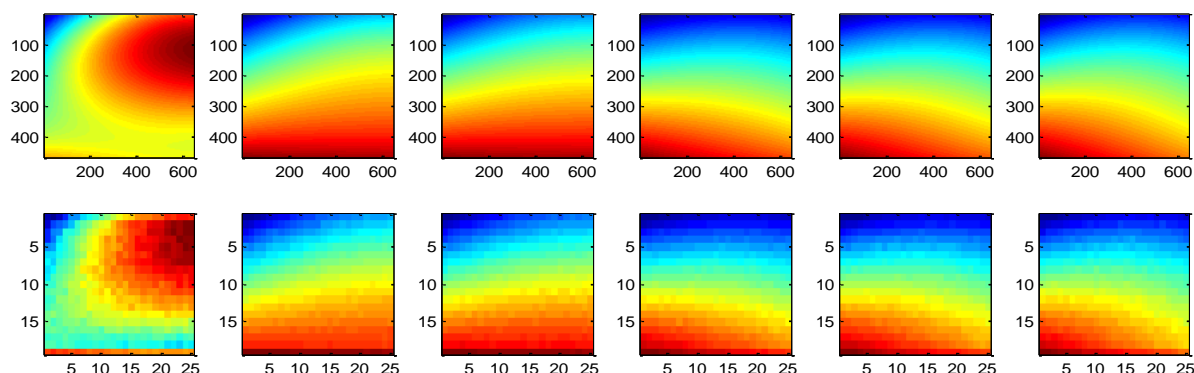


**Figure 5: approximation of the deviation versus discrete sampling points beginning from the 400nm channel up to 650nm channel, upper pictures displaying the approximation on the complete image lower images displaying the discrete sampling points of the detected circles;**

In order to implement this algorithm in a smart spectral imager, the correction values are placed in a digital filter core which moves over the distorted picture and is actualized with for every new incoming pixel. Formal a linear folding operation with changing coefficients is applied to correct the distorted images. The big advantage is that only the filter core has to be updated during an incoming image. The size of the core depends on the absolute value of error and has an odd core size. For the used lens the absolute value of the deviation is nine pixels. The deviation is direction dependent that leads to the effective size of the filter core. In this case the dimension is nine. The deviation based on the optical distortions, leads to a non-raster synchron movement. For this reason the integral assumption of four pixels were applied. Therefore it is assumed that the pixel intensity is divided in four pixels hugely (Figure 6).

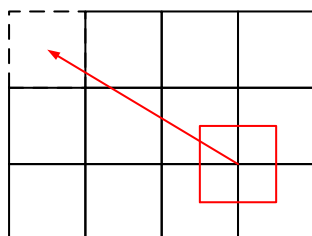


**Figure 6: example for an uniformly distributed pixel, in this case a quarter intensity of the four pixel were used;**

To move the gray value on the correct position two pixels in x and two pixels in the y direction which were weighted with the position values. That leads to the usage of a maximum of four pixels.

#### 4. Results

After the analysis and the processing of the data, Figure 7 shows the results of the correction on the calibration target. With the applied method a deviation less than a half pixel can be achieved. In Figure 7 part d.) the uncorrected data along the search line is displayed. The difference between the edge transitions over all channels has a deviation of nine pixels between the different wavelength channels.

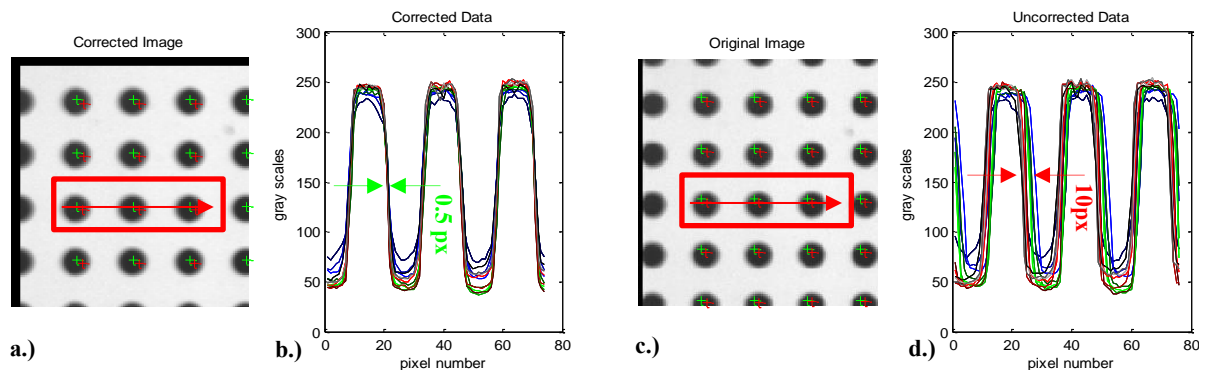


**Figure 7:** a.) corrected image the green crosses (expected position without errors) are in the centre of the circle after correction (channel 4, 550nm), b.) edge transition of the corrected images (left), c.) detected centre of the circles (red crosses) (channel 4, 550nm), d.) edge transition uncorrected; (blue graphs 400-500nm, green graphs 550-650nm, red graphs 700-800 nm, grey scaled graphs 850-950nm);

With the used lens and the applied correction algorithm a deviation of less than 20 microns at a field of 20000x26000 microns in all channels is achievable. For geometric detection a decrease of a factor of ten in uncertainty is possible with the correction. Furthermore multi-channel edge detection algorithms will deliver better results.

## References

- [1] F. König and P. Herzog, "On the limitations of metameric Imaging", Proceedings of IS&T PICS, 1999, pp. 163-168.
- [2] M. Yamaguchi, H. Haneishi, and N. Ohya, "Beyond Red-Green-Blue (RGB): Spectrum-based color imaging technology," J. Imag. Sci. Technol., vol. 52, no. 1, pp. 010 201-1–010 201-15, Jan. 2008
- [3] M. Preißler, M. Rosenberger, M. Correns, M. Schellhorn and G. Linß, „Investigation on a modular high speed multispectral camera“, Proceedings of the 20th IMEKO TC2 Symposium on Photonics in Measurement : May 16 - 18, 2011, [Linz Austria], pp.59-62, Aachen : Shaker, 2011.
- [4] M. Preißler, M. Rosenberger, G. Linß: "Smart Spectral Imager", 2012 IEEE Photonics Conference (IPC 2012) : Burlingame, California, USA, 23 - 27 September 2012. - Piscataway, NJ : IEEE. - 2012, S. 591-592
- [5] H. Haferkorn: "Bewertung optischer Systeme", Berlin : Dt. Verl. der Wiss., 1986, ISBN 3-326-00000-6